

**Restructuring of
a zooplankton community
by perturbation from
a wind-forced coastal jet***

OCEANOLOGIA, 52 (3), 2010.
pp. 473–497.

© 2010, by Institute of
Oceanology PAS.

KEYWORDS
Zooplankton
Filament
Intrusion
Restructuring
Mesoscale

OLE-PETTER PEDERSEN^{1,*}
KURT S. TANDE²
CHAOLUN LI³
MENG ZHOU⁴

¹ University of Tromsø,
9037 Tromsø, Norway;
e-mail: ole.p.pedersen@uit.no

*corresponding author

² Bodø University College,
8049 Bodø, Norway

³ Institute of Oceanology,
Chinese Academy of Sciences,
266071 Qingdao, P. R. China

⁴ Department of Environmental, Earth and Ocean Sciences,
University of Massachusetts,
Boston, MA 02125, USA

Received 2 June 2010, revised 23 September 2010, accepted 26 August 2010.

Abstract

The impact of transient wind events on an established zooplankton community was observed during a field survey in a coastal region off northern Norway in May 2002. A transient wind event induced a coastal jet/filament intrusion of warm, saline water into our survey area where a semi-permanent eddy was present. There

*This work was supported by the Research Council of Norway, contract No. 140290/140.

was an abrupt change in zooplankton community structure within 4–7 days of the wind event, with a change in the size structure, an increase in lower size classes less than 1 mm in equivalent spherical diameter (ESD) and a decrease in larger size classes greater than 1.5 mm in ESD. The slope of zooplankton biovolume spectra changed from -0.6 to -0.8 , consistent with the size shifting towards smaller size classes. This study shows that even well established zooplankton communities are susceptible to restructuring during transient wind events, and in particular when wind forcing induces horizontal currents or filaments.

1. Introduction

The role of mesoscale eddies in modifying the physical, chemical and biological environment in the ocean is well documented (Mann & Lazier 2006, Eden et al. 2009). Since mesoscale processes may be linked to the supply of nutrients and elevated productivity, such research has been carried out in oligotrophic systems (McGillicuddy et al. 2007, Benitez-Nelson et al. 2007). Eddies are important in structuring marine planktonic communities through their influence on nutrient availability and the subsequent biological response (Owen 1981), but there are relatively few studies on eddy-induced changes in the zooplankton community (Davis & Wiebe 1985, Hernández-León et al. 2001, Tsurumi et al. 2005, Goldthwait & Steinberg 2008, Landry et al. 2008, Eden et al. 2009). It was concluded from these studies that significant changes in food-web structure and biomass at the zooplankton level were found in eddies that persist significantly longer than the generation time of dominant zooplankton species.

The translation, size, durability and internal dynamics of eddies found on or adjacent to shelves show large variability. All along the Norwegian coast, mesoscale eddies are often generated by the meandering of the front between Norwegian Coastal Water (NCW) and Atlantic Water (AW) (Figure 1) (Sundby 1984, Johannessen et al. 1996). Recent studies have shown that eddies are associated with bottom topography, wind and tidal forcing, and, where situations permit, can have a horizontal translation speed of several kilometres per day (Pedersen et al. 2005). Previous studies found strong correlations between mesoscale eddies and topographic features (Ljøen & Nakken 1969, Zhu et al. 2009). Shelf waves, wind-driven currents, runoff-induced density currents and topography-induced jets all have great influence on the size and duration of eddies, subsequently affecting the biological regime within the eddies (Sætre & Ljøen 1971, Gjevik & Moe 1994, Orvik & Mork 1995, Ottersen & Sundby 1995, Fossheim et al. 2005).

In a recent study of mesoscale physical processes and the transport and retention of zooplankton on the North Norwegian shelf, Zhu et al. (2009) found that the coastal currents played an important role in both the northward transport and the local retention of zooplankton. Areas of

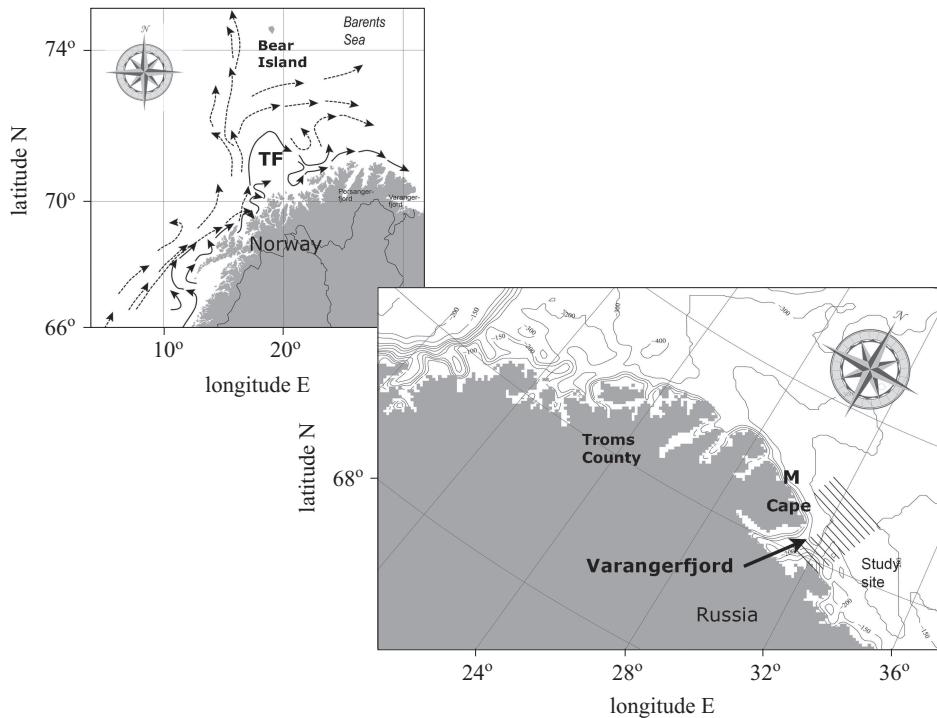


Figure 1. Upper panel: Idealized surface circulation map of the study area. Stippled arrows denote the Norwegian Atlantic Current and solid arrows denote the Norwegian Coastal Current, TF – Trosøflaket. Lower panel: Map of northern Norway depicting the study area. The parallel lines are the survey transects. ‘M’ denotes the Makkaur meteorological station

high zooplankton abundance occurred locally through retention by physical processes and in particular recurrent eddy formation, but variable small- and mesoscale currents would also cause significant horizontal dispersion of zooplankton. The study showed that the local retention of zooplankton through horizontal transport was significant and of the same order of magnitude as the local productivity contributed to by individual growth.

The objective of this study is to understand how external drivers like wind events can modify an eddy and restructure the zooplankton community and feeding habitat for fish larvae. It was carried out as part of the Barents Sea Capelin and Herring – Coexistence or Exclusion (BASECOEX) research programme studying the spawning and larval habitat of capelin (*Mallotus villosus*) during spring 2002.

This study reports on the physical and biological eddy structure off the Varanger peninsula in northern Norway prior to and after perturbation from a wind-forced coastal jet and undertakes an in-depth analysis of how wind

events modify advection and retention in an eddy during the most intensive growth and recruitment period of zooplankton and ichthyoplankton in north Norwegian waters.

2. Method

2.1. Selection of the survey area

The survey area for this study was chosen on the basis of previous work in the region. Recent studies report that cyclonic eddies off the Norwegian coast contain oceanic waters and abundant zooplankton, whereas anticyclonic eddies contain coastal waters and less abundant zooplankton (Fossheim et al. 2005). A relatively stable eddy region was previously identified (Pedersen et al. 2009) at the mouth of Varanger fjord (Figure 1) and was adopted as the study site for this investigation into coupled physical, primary production and trophic dynamics of higher-level organisms within a stable eddy.

The Varanger fjord is open to the east with a width of over 40 km and a depth of over 230 m. A prominent headland, hereafter referred to as ‘the Cape’, is a striking feature of its northern shore. Off the Cape, the shelf is narrow, sloping down to below 350–400 m within 15 km. Such topographic features steer the coastal currents and frequently generate eddies. The survey area was specifically selected on the basis of prior information on retention fields formed by eddies and coastal currents, and because high concentrations of capelin larvae were found here (Pedersen et al. 2005, 2009, Pedersen & Fossheim 2008).

2.2. Prevailing current system

Along the Norwegian coast, two major current systems dominate: the Norwegian Atlantic Current (NAC) and the Norwegian Coastal Current (NCC) (Figure 1). The NAC enters the Norwegian Sea through the Faeroe-Shetland Channel, containing AW. Within the NCC, the Norwegian Coastal Water (NCW) originates primarily from the fresh water outflow from the Baltic Sea and freshwater discharge from Norway. The NCW is characterized by salinities and temperatures lower than 34.5 and 5.5°C (Ljøen & Nakken 1969). Further north, at about 10–20°E outside Troms County, the NAC splits. One branch follows the continental shelf edge northwards while the other branch flows around Tromsøflaket and continues along the Norwegian coast. These two bodies of water are present and interact in our study area. The current system along the coast of northern Norway is complex, and rich in mesoscale eddies. This is mainly due to the intricate bathymetry, including banks, canyons and fjords. The bottom

depth changes abruptly from 10 to 400 m within a short distance at several locations. Superimposed on bathymetric steering and interaction between water masses are atmospheric drivers. Wind produces onshore or offshore transport, coastal upwelling and downwelling, and barotropic and baroclinic coastal currents (Price et al. 1987).

2.3. The field campaign and instrumentation

The mesoscale hydrographic, current and zooplankton fields in the study region were sampled twice on board the r/v 'Jan Mayen' in the periods between 15 and 17 May 2002 with 13 transects and between 21 and 22 May 2002 with 11 transects. For each period, the survey times and details of each transect are provided (see Table 1). The sampling was carried out using an Optical Plankton Counter (OPC; Focal Technologies Inc., Dartmouth, Canada) and a CTD (Sea-Bird 911; Sea-Bird Electronics Inc.,

Table 1. Survey time (UTC) of each transect in Period 1 and Period 2*

	Transect	Date	Start	Stop
Period 1	S1	15.05.2002	17:18	19:24
	S2		19:49	21:42
	S3		22:07	23:59
	S4	16.05.2002	00:24	02:20
	S5		02:44	04:23
	S6		04:48	06:31
	S7		06:56	08:46
	S8		09:15	11:16
	S9		11:44	15:44
	S10	17.05.2002	16:09	19:58
	S11		23:58	03:58
	S12		04:18	07:54
	S13		08:27	12:22
Period 2	S3	21.05.2002	01:07	03:15
	S4		03:35	05:39
	S5		05:39	07:57
	S6		08:21	10:12
	S7		10:38	12:33
	S8		13:07	15:24
	S9	15:51	19:51	
	S10	22.05.2002	20:13	00:08
	S11		00:41	04:38
	S12		05:02	08:55
	S13		09:22	13:08

*Sunset was at 22:24 and sunrise at 23:21 on 15 May 2002. After this date the sun did not set during the survey period.

Washington, USA), both of which were mounted on a SCANFISH towed instrument platform (MKII SCANFISH, GMI, Snekkersten, Denmark). This instrument platform was towed behind the ship at a speed of 6 knots while undulating from 5 to 100 m at an average undulating speed of 0.5 m s^{-1} .

After each survey period, the hydrography and zooplankton were also sampled by using traditional CTD casts and a Multiple Opening and Closing Net and Environmental Sensing System (MOCNESS; Wiebe et al. 1985) respectively, at nine stations located inside the survey area for the ground truthing (Figure 2a).

2.4. Data processing

Data from the CTD and OPC were processed and integrated into one dataset containing latitude, longitude, date, time, temperature, salinity, and zooplankton abundances and biovolumes within 60 size classes. The details of data processing for salinity, temperature and density can be found in Pedersen et al. (2005). In brief, we divided the water column into 5 m depth bins along the Scanfish trajectories. For interpolation and smoothing of the measured field, Objective Analysis (OA) was applied (Gandin 1963). On the basis of the processed density fields, we calculated the relative geostrophic currents for the entire water column using 100 m as the reference layer since the maximum sampling depth was 100 m.

The OPC counts particles in 4096 digital sizes within a range of 0.25–24 mm Equivalent Spherical Diameter (ESD) (Herman et al. 2004). This size range is composed predominantly of zooplankton, so hereafter we refer to the particles as zooplankton. With the flow speed measurements by a GO flowmeter (General Oceanics, USA) mounted underneath the OPC, zooplankton counts were normalized by the volume filtered to abundance (individuals m^{-3}) within 60 size classes of equal log (ESD) increments. The OPC data were regrouped into 4 ESD size ranges: 0.25–1.00, 1.00–1.40, 1.40–2.00 and > 2.00 mm, hereafter named Small, Medium, Large and XL zooplankton. These size groups are arbitrary, although they approximately represent *Calanus finmarchicus* C1–2, C3–4, C5–f and other large zooplankton, in accordance with information on ESDs of the dominant zooplankton species in this region obtained from the MOCNESS tow samples (Pedersen et al. 2010).

The spherical body volume of a zooplankter was computed directly from the ESD measurement by an OPC. Assuming the specific wet weight to be 1 g cm^{-3} , this body volume is equivalent to the wet weight body biomass (Wiebe 1988). The relationship between the body carbon weight and the wet weight can vary in different species (Rodriguez & Mullin 1986, Wiebe

1988). Though these empirical wet weight and carbon relationships can be used as a first order of approximation, we simply use the body volume equivalent to the body wet weight in the rest of this article.

For the presentation of horizontal and vertical zooplankton distributions, we first calculated the accumulative zooplankton body volume and counts in each 5 m depth bin normalized by the water volume filtered, referred as to biovolume and abundance in $\text{mm}^3 \text{m}^{-3}$ and individuals m^{-3} respectively. These data were then horizontally interpolated across our survey grid using the OA method (Gandin 1963).

To further explore the zooplankton population dynamics, the biovolume spectrum (equivalent to the biomass spectrum) was computed on the basis of 60 size classes in each 5 m depth bin using the standard definition (Platt & Denman 1978), i.e.

$$\text{Biovolume spectrum } (b) = \frac{\text{biovolume in the size interval } (\Delta v)}{\text{the size interval } (\Delta v)} [\text{m}^{-3}] \quad (1)$$

where the size (v) of a zooplankter is the body volume in mm^3 . As a cohort of zooplankton grows from small to large, the number of zooplankton organisms decreases as a result of mortality. Thus, most in situ zooplankton observations show a monotonic decrease in abundance from small to large sizes (Dickie et al. 1987, Zhou 2006). If the mortality is caused by predation, i.e. smaller animals being grazed by larger ones, the slope of the biomass spectrum represents the foodweb structure, or the biomass transfer from small to large organisms through predation. On the basis of temporal changes in biomass spectra, growth and mortality rates can be estimated as a function of body size (v) (Edwardsen et al. 2002, Zhou 2006). To assess the trophic dynamics based on zooplankton size structure, in this study we calculated the mean slopes of the biovolume spectra representing the plankton community structures between different water masses or regions based on the theories provided by Dickie et al. (1987) and Zhou (2006). To obtain this overall mean slope of the biovolume spectrum, we used a linear function to fit the observed spectrum.

3. Results

3.1. Conditions before the coastal jet intrusion (Period 1)

The physical mapping showed a number of mesoscale physical features in the survey region, with a residual flow from the west to the east/south-east, turning sharply at the Cape (Figure 2).

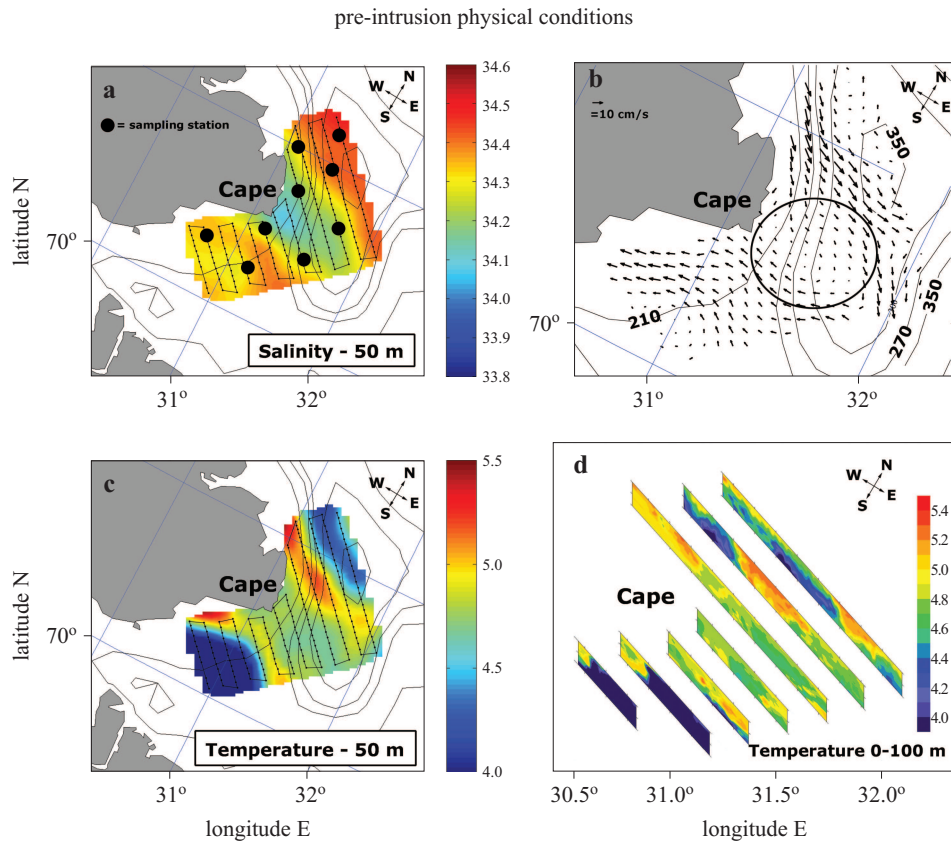


Figure 2. Physical conditions during Period 1 (pre-intrusion). a) Salinity at 50 m, black dots show MOCNESS sampling stations. b) Currents at 50 m, c) temperature at 50 m and d) temperature throughout the upper 100 m

3.1.1. Hydrography

During Period 1, in the northern part of our study region, there was a fast, along-shelf geostrophic current entering the survey area from the north-west, crossing the deep basin and exiting to the east (Figure 2b). A fast, shoreward geostrophic current entered the survey area from the SE and was deflected to the west along the coast. These opposing currents were associated with a mesoscale anticyclonic eddy on the slope off the Cape (Figure 2b, circle). The current reached a maximum velocity of approximately 25 cm s^{-1} at the surface along the shelf edge in the north, and decreased to nearly zero in the interior of the eddy. There was also a general decrease in the current velocity with depth (not shown here), diminishing at the reference depth of 100 m. The circulation pattern observed is well

conserved throughout the water column, and is persistent down to 100 m, which is our maximum sampling depth.

The water inside the eddy was relatively fresh ($S < 34.3$), while the surrounding water to the north and south (Figure 2a) had a higher salinity ($S > 34.3$). To the south of the study region, the water was relatively saline and cold (Figures 2a,c). This signature is typical of Norwegian Deep Fjord Water (NDFW), characterized by $34.3 < S < 34.5$ and $T < 4^\circ\text{C}$. The longshore current in the north is warm and saline (Figures 2a–d). This is AW ($3 < T < 7^\circ\text{C}$, $S > 34.5$) that has been cooled and diluted along the Norwegian coast (Loeng 1991). To the north of this warm, saline current there is a colder and more saline cushion. The vertical transects of temperature show that the water off the Cape is the warmest in the survey area and was clearly associated with the longshore current (Figure 2d). A TS-plot from Period 1 (Figure 3a) demonstrates that the waters in the survey area consist of AW modified by the local NCW and heat loss, and a unique cold NDFW, whose formation is associated with winter cooling and ice formation.

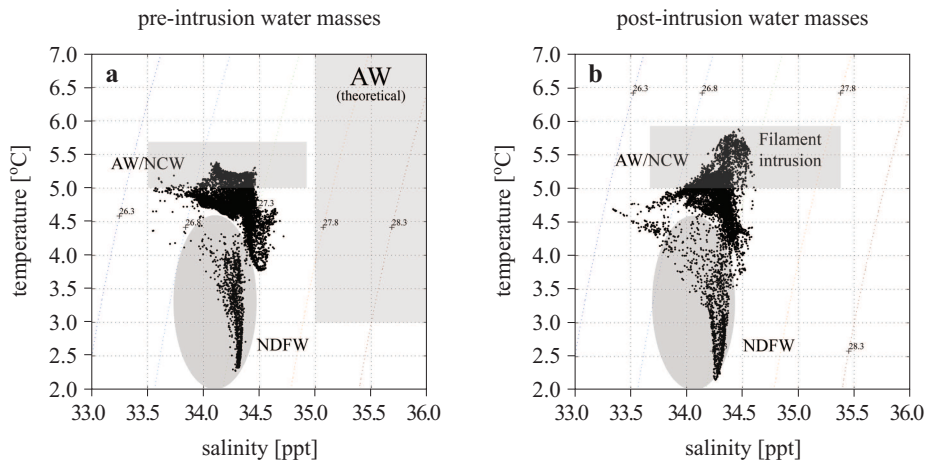


Figure 3. Temperature and salinity plots for Period 1 (pre-intrusion) and Period 2 (post-intrusion)

3.1.2. Distribution of zooplankton

The vertically-integrated zooplankton abundance (individuals $\times 10^3 \text{ m}^{-2}$) above 100 m shows two maxima, one in the northern part of the study area associated with the fast flowing longshore current and one in the southern part of the study area associated with NDFW (Figure 4a). The zooplanktonic communities represented by size groups were mapped

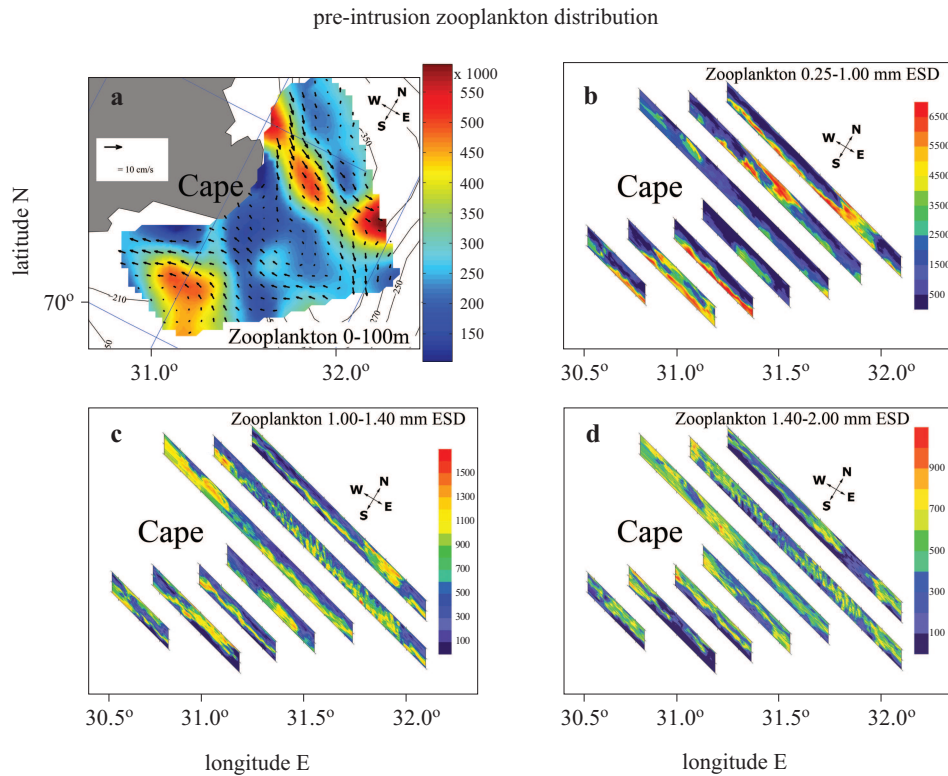


Figure 4. Pre-intrusion zooplankton distribution. a) Integrated zooplankton abundances (indiv. $\times 10^3 \text{ m}^{-2}$) above 100 m. b) Abundance of small zooplankton (indiv. m^{-3} , 0.25–1.00 mm ESD). c) Abundance of medium zooplankton (indiv. m^{-3} , 1.00–1.40 mm ESD). d) Abundance of large zooplankton (indiv. m^{-3} , 1.40–2.00 mm ESD)

vertically along the survey transects (Figures 4b–d). The small zooplankton (0.25–1.0 mm in ESD) were dominant with respect to abundance (> 6500 individuals m^{-3}) and was generally located in deeper depth strata (Figure 4b). The medium-sized zooplankton (1.0–1.4 mm in ESD) were concentrated in the water column above the small zooplankton with the greatest abundances at 20–50 m (Figure 4c). However, the spatial distribution was far more dispersed with very few identifiable hotspots, and the abundance was less than 1700 individuals m^{-3} . The large zooplankton size group (1.4–2.0 mm in ESD) was found to contain less than 1100 individuals m^{-3} in the entire area (Figure 4d). Generally, they were homogeneously distributed in our survey area and throughout the water column. However, the abundance was slightly greater in the coastal area off the Cape. The numbers of XL zooplankton (> 2.00 mm ESD) were less

than 300 individuals m^{-3} and were much less abundant than those in the smaller size groups (not shown).

3.2. Wind forcing and induction of the coastal jet

The intrusion of new water masses was linked to a significant change in local wind patterns. The wind magnitude and direction data collected during the survey period at the Makkaur meteorological station by the Norwegian Meteorological Institute (<http://www.eKlima.no>) are shown in Figure 5, indicating a significant change of wind magnitude and direction between survey periods 1 and 2 (Figure 5). The wind surge lasted for nearly 3 days. The prevailing direction changed from NE to N/NW, and the magnitude increased significantly. A N/NW wind will induce transport in the SW direction (in close resemblance to Ekman theory), which is also consistent with the direction of the filament intrusion observed in Period 2 (Figure 2c vs. Figure 6c). The duration of the storm surge was approximately 3 days, during which a steady Ekman type flow could be produced (Lewis & Belcher 2004).

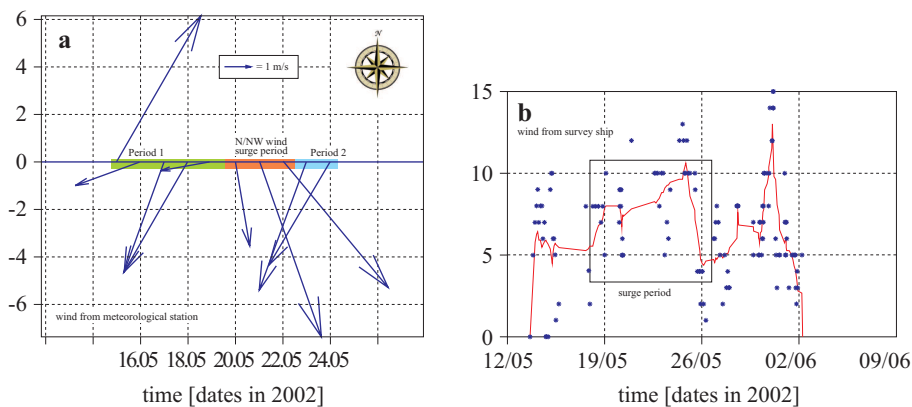


Figure 5. a) Diagram of wind magnitude and direction during the survey obtained from a land based meteorological survey point (Makkaur) marked by ‘M’ in Figure 1. b) Wind magnitude sampled from the survey ship. The black rectangle identifies the surge period and the red line is the moving average

3.3. Conditions after the coastal jet intrusion (Period 2)

The major changes observed after the wind event were the filament intrusion of warm water from the north and the presence of two eddy features (Figure 6), contrasting with the single eddy found in Period 1 (Figure 2).

3.3.1. Hydrography

In Period 2, some of the features seen during Period 1 were still present (Figure 6), but two anticyclonic mesoscale eddies had developed with weak currents extending down to approximately 50 m depth (Figure 6b, circles). One was close to the Cape, while the other was located at the eastern border of the survey area. The development from one single eddy in Period 1 (Figure 2b) to two in Period 2 is due to the observed filament intrusion from the north (Figures 2c and 6c), i.e. eddy splitting. The vertical transects of the temperature show that the whole Cape region is warmer than the northern and southern sides of the survey region, although the temperatures are elevated compared to Period 1 (Figure 6d). The TS-plot from Period 2 also shows the presence of warmer water masses related to the filament intrusion (Figure 3b).

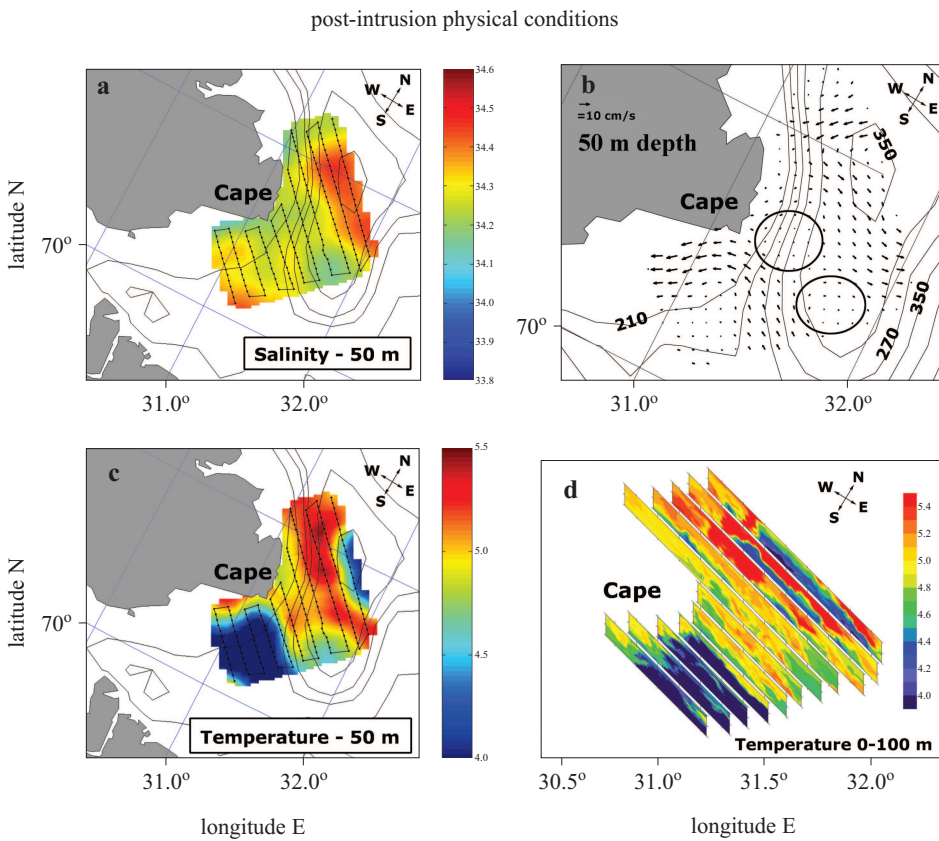


Figure 6. Physical conditions during Period 2 (post-intrusion)

3.3.2. Distribution of zooplankton

The abundance of zooplankton in the study area increased significantly from Period 1 to Period 2 (Figures 4a and 7a). The abundance of small zooplankton (0.25–1.0 mm ESD) increased on the northern and southern fringes of the survey area (Figure 7b). The medium zooplankton size group (1.00–1.40 mm ESD) remained heterogeneously distributed all over the survey area (Figure 7c), which is consistent with the pre-intrusion conditions (Figure 4c), although there was a general increase in abundance. With respect to the large zooplankton (1.40–2.0 mm ESD), there was an apparent shift in spatial distribution. The heterogeneous distribution from Period 1 changed into a much more confined pattern, located in the centre

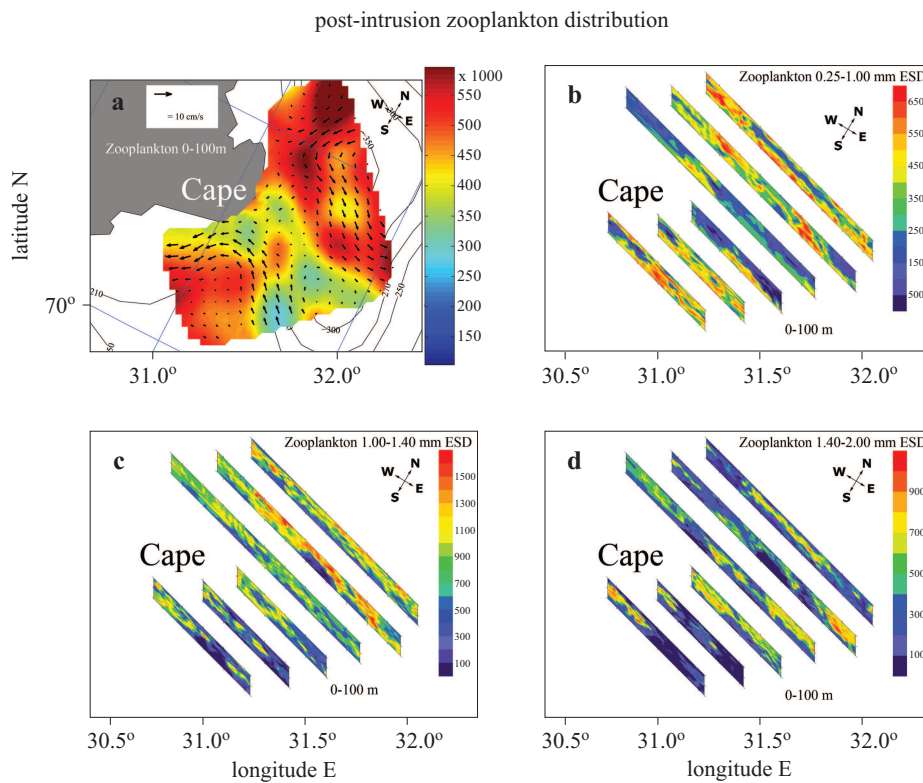


Figure 7. Post-intrusion zooplankton distribution. a) Integrated zooplankton abundances ($\text{indiv.} \times 10^3 \text{ m}^{-2}$) above 100 m. b) Abundance of small zooplankton (indiv. m^{-3} , 0.25–1.00 mm ESD). c) Abundance of medium zooplankton (indiv. m^{-3} , 1.00–1.40 mm ESD). d) Abundance of large zooplankton (indiv. m^{-3} , 1.40–2.00 mm ESD)

of the survey area (Figures 4d and 7d). There is a very interesting spatial characteristic which can be observed in Period 2: small zooplankton and large zooplankton show distinctive complementary spatial distributions, i.e.

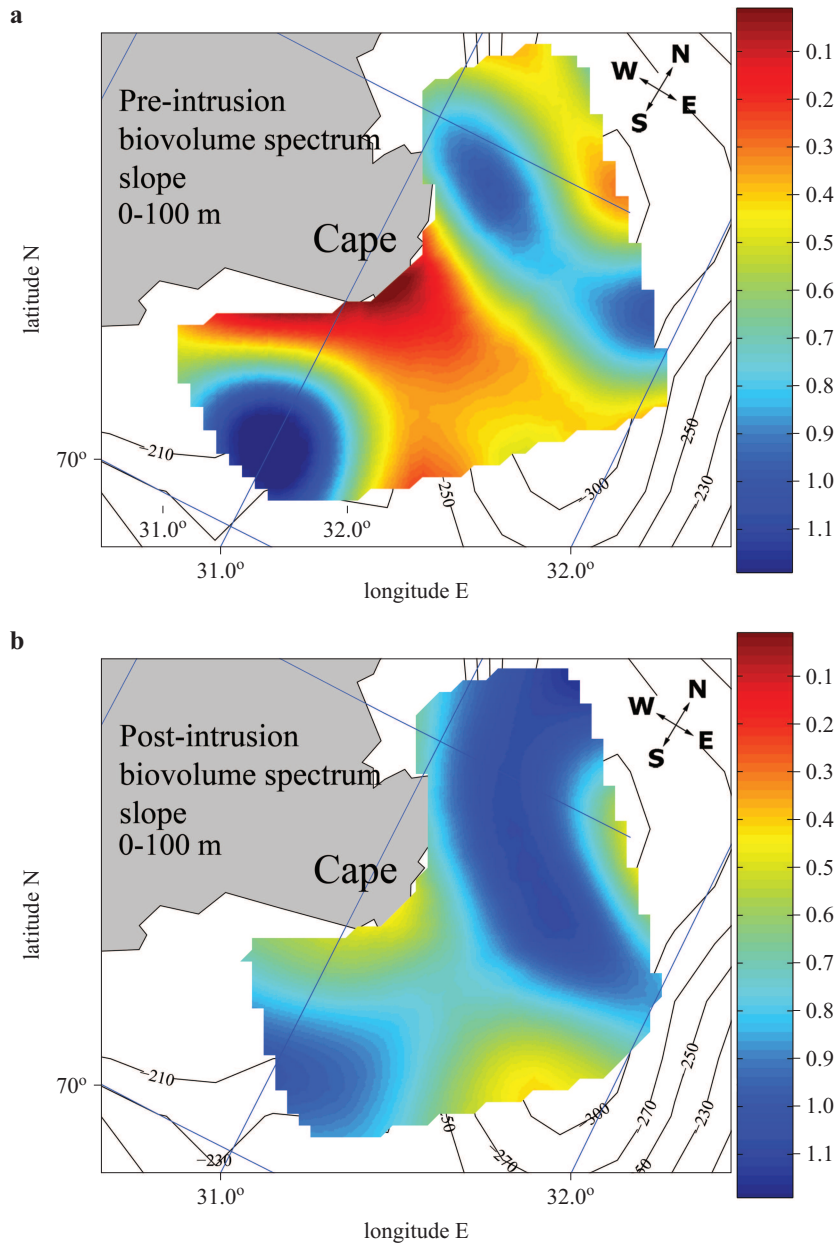


Figure 8. Horizontal distribution of the slopes of zooplankton biovolume spectra during a) Period 1 and b) Period 2

the northern and southern flanks of the survey area were populated by smaller forms (0.25–1.0 mm ESD), while the centre was populated by larger forms (1.40–2.0 mm ESD).

3.4. Biovolume spectrum – before and after perturbation by the coastal jet

To study the spatial difference of zooplankton size structure, the slopes of the zooplankton biovolume spectra were calculated in each 0.1° longitudinal bin of all transects (Figures 8a,b). During Period 1, the slopes in the retention field south-east of the Cape were relatively flat compared to further north and south (Figure 8a). In Period 2, after the intrusion of the coastal jet, the number of high-value slopes had decreased all over the survey area, and the maximum value of the slope had dropped to -0.4 (Figure 8b). For both periods, the minimum value was approximately -1.1 . The horizontal distributions of the slopes show patterns that are remarkably similar to those of zooplankton abundances. This is particularly evident if Figure 4a is compared with Figure 8a (Period 1), and Figure 7a with Figure 8b (Period 2). As a rule, an increase in the abundance of larger zooplankton gives a less steep slope, while an increase of smaller zooplankton will steepen it.

The detailed zooplankton size spectra for both periods are shown in Figure 9. The interesting points are the changes that took place between the two sampling periods. The numbers of small/medium zooplankton (< 1.5 mm) increased, while the numbers of medium size/large zooplankton

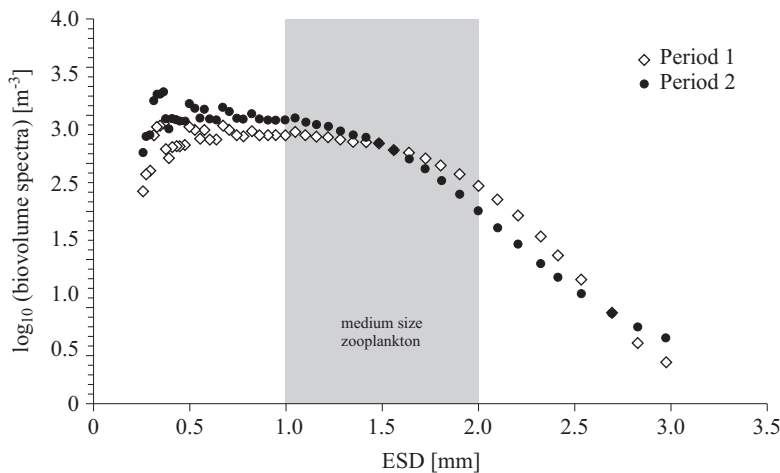


Figure 9. Biovolume size spectra before (Period 1) and after (Period 2) the intrusion event

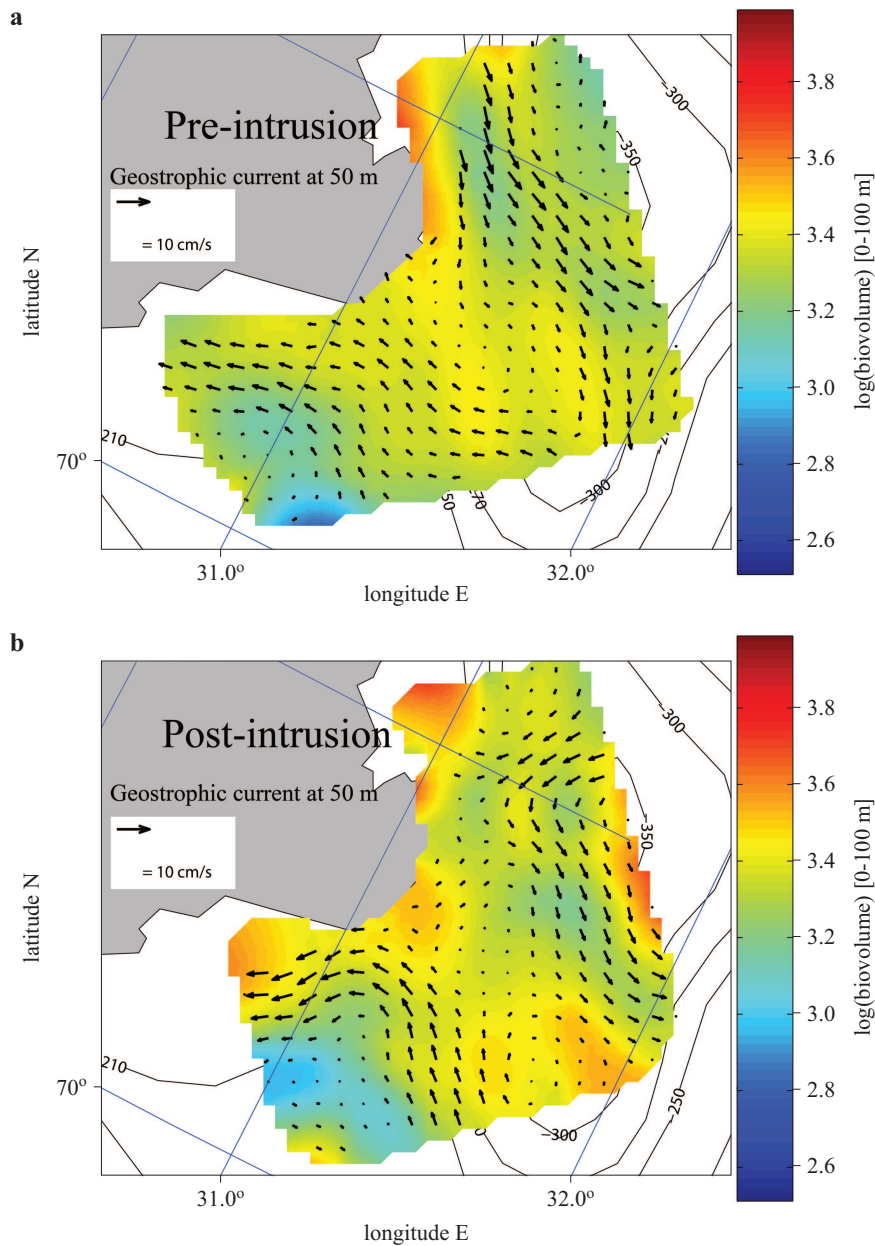


Figure 10. Logarithmic values of the average zooplankton biovolume [$\text{mm}^3 \text{m}^{-3}$] above 100 m before and after the intrusion event

(1.5–2.5 mm) decreased. The mean slope decreased from -0.6 to -0.8 from Period 1 to Period 2. There appears to have been a shift in the community structure, in which the size distribution shifted towards smaller

size intervals. What this implies, apart from the face value of the change, will be discussed further. In general, zooplankton are exposed to a number of external and internal processes (e.g. advection, predation, growth, mortality and vertical migration), but the actual impact of each one in time and space is still to be addressed. In systems with a high variability in current magnitude and direction, e.g. tidally dominated shelf areas, the retention rate is low, and the dominance of advection is high. In less energetic regions (e.g. offshore areas, bays, semi-enclosed estuaries or fjords), growth and mortality will have stronger effects on changes in zooplankton population structures. This is further addressed in the discussion. Integrating the spatial biovolume fields over the whole ESD range before and after the perturbation by the wind-forced coastal jet (Figure 10) demonstrates a build-up of biovolume in the central region. The data presented in Figure 10 are \log_{10} -transformed. A change from 3.4 to 3.6 in log-space equals an increase of approximately 60% in the biovolume. This is also corroborated by comparison of Figures 4a and 7a.

4. Discussion

This study confirms that there is a semi-permanent topographically steered eddy at the shelf off Varanger in Finnmark, northern Norway. The analysis identified several general trends in our survey area with respect to circulation and hydrographic conditions. Three different features are particularly prominent. First, the presence of a retention field in the middle of our survey area, indicating a consistent, possibly permanent, site for the retention and aggregation of zooplankton and fish larvae. Supporting this observation is local information from fisheries communities and previous scientific studies, claiming large concentrations of fish, sea mammals and birds in this region (Jakobsen 1987).

Secondly, the presence of a strong longshore current, transporting mesoscale eddies and passive biota downstream. This current is part of the NCC and makes a sharp turn into the local fjord system (Varanger) on the southern fringe of our survey area, probably steered by the shelf slope. A previous study along the coast of northern Norway, east of this study site, documented elevated abundances of zooplankton in eddies with Atlantic water masses (Fossheim et al. 2005). These features were identified upstream of the survey area in the present study. During the advection of these eddies they were elongated in the along-shelf direction. Being carried downstream, at a certain point they reached the offshore side of our survey area, and translated around the semi-stable eddy in accordance with the prevailing physical forcing.

Thirdly, this work identifies the occurrence of intrusive filaments, as a direct response to episodic wind events. Periodic wind events are very likely to set up temporary surface currents, as in the present case, as a warm, intrusive filament transporting a high abundance of zooplankton into local retention fields off Varanger. This investigation highlights the strong interaction between wind forcing and coastal jets, consequently with significant effects on advection of zooplankton communities. That makes loss rates and retention particularly susceptible to wind forcing, with a stochastic nature since wind events do not occur on a regular basis.

The coastal jet was identified as an intrusion of water masses of Atlantic origin, mirrored by a shift in the abundance and size structure of zooplankton, and resulting in an increase in total zooplankton abundance in the local retention area off Varanger. The shift in size distribution showed an increase of smaller sizes, while larger size groups declined. This clearly demonstrated the shift in the size and biovolume spectra prior to and after the wind event. The biomass (and biovolume) spectrum has proven to be a valid approach for documenting zooplankton community dynamics. As zooplankton cohorts grow in size, depressions or peaks can be identified from the biovolume spectra propagating along the size axis (Edvardsen et al. 2002). Without advection, the change in a biovolume spectrum can be used to infer mortality that moves the biovolume spectrum downwards, and individual growth that moves the biovolume spectrum to the right. The intercept of the curve represents abundance, while population processes like growth and mortality are attributed to the slope. Additional details on the relationship between population parameters and biovolume spectra, including the factors that cause spatial-temporal changes in the slope of the spectra, are available in Zhou (2006) and Zhou et al. (2009).

Since the zooplankton community was composed of the same species and stages throughout our survey period (Tables 2 and 3), the size and abundance values from a biovolume spectrum therefore represent the in situ changes in abundances of zooplankton species and stages between the periods. The numbers are given as after sampling Period 1 and after sampling Period 2. The zooplankton assemblages were dominated by copepods in both survey periods, making up 78/61% of the total abundance in the study area as derived from analysis of the MOCNESS samples. The copepods were mainly *Calanus finmarchicus* (45/51%), copepod nauplii (33/10%), *Oithona* spp. (8/16%) and *Metridia* spp. (2/3%). Other groups were *Oikopleura* spp. (4/10%), euphausiids (5/3%), echinoderm larvae (2/6%) and capelin larvae (~1%) (Table 3). The most dominant changes in the zooplankton assemblages between Periods 1 and 2 were the early *C. finmarchicus* stages (CII–CIV) (Table 4). The increase in abundances of CII–CIV

Table 2. Number-dominant species of zooplankton in Period 1 and 2 from the MOCNESS

Size group	ESD [mm]*	Species
small	0.25–1.00	<i>Calanus finmarchicus</i> CI–III
		<i>Copepod nauplii</i>
		<i>Oithona</i> spp.
		<i>Metridia</i> spp.
medium	1.00–1.40	<i>Calanus finmarchicus</i> CIII, CIV
		<i>Oikopleura</i> spp.
		Capelin larvae
large	1.40–2.00	<i>Calanus finmarchicus</i> CV, Ad
		<i>Euphausiacea</i> larvae
xlarge	> 2.00	<i>Euphausiacea</i>

* The zooplankton ESD values were based on data from Edvardsen et al. (unpublished data).

Table 3. Species distribution in Period 1 and 2 from the MOCNESS

Species	Period 1, percentage distribution	Period 2, percentage distribution
<i>Calanus finmarchicus</i> CI–Ad	45	51
Copepod nauplii	33	10
<i>Oithona</i> spp.	8	16
<i>Metridia</i> spp.	2	3
<i>Oikopleura</i> spp.	4	10
Euphausiids	5	3
Echinoderm larvae	2	6
Capelin larvae	1	1
other species	0	0

of CII–CIV is reflected in the general mapping of total abundances in the area (Figures 4 and 7), the changes in the horizontal distributions of the slopes (Figure 8) and the biovolume size spectra (Figure 9).

We observed a large transport of small organisms (< 1.5 mm) into the survey area, and consequently a change in the biomass spectrum slope. The observed upward movement of the spectrum between 0.3 and 1.5 mm in ESD is interpreted as the additional small zooplankton advected in by the Ekman current intrusion, and a decrease in size larger than 1.5 mm in ESD can only be contributed to by mortality (Figure 9). This is an average for

Table 4. Copepod abundance and change between Period 1 and 2

<i>Calanus finmarchicus</i>	Period 1, abundance [$\# \text{ m}^{-3}$]	Period 2, abundance [$\# \text{ m}^{-3}$]	Change [%] between Period 1 and 2
CI	5369	4821	-10
CII	3451	6362	84
CIII	1726	4453	158
CIV	826	2002	143
CV	253	620	145
female	97	107	10
male	10	6	-41

the entire survey area. However, in order to study spatial patterns, we also calculated the distribution of the slopes covering the entire survey area, and the change in the distribution before and after the perturbation from the wind-forced coastal jet. The spatial distribution of the slope of the biomass spectrum declined throughout the entire survey area. In the pre-intrusion period, the central study area had a slope in the range of -0.1 to -0.6 , with a subsequent steepening to -0.5 to -0.8 after the intrusion event.

The biomass spectrum theory suggests that this indicates a change in community structure, which becomes more herbivorous with more smaller zooplankton after the intrusion, and leading to a reduction in the number of trophic levels and a lower degree of recycling (Zhou et al. 2009). The organisms transported into the region were in the size range of 0.25–1.4 mm ESD. Since ca 84% of the observed biomass were copepods (Table 2), we infer that the size range introduced comprised more young stages such as nauplii and young copepodites, usually N1–N6 and CI–CIV. These are predominantly herbivorous stages compared to the more advanced copepodites; hence it is reasonable to assume a community shift towards more herbivorous grazing in the post-intrusion period compared to a more carnivorous/omnivorous composition in the pre-intrusion period. This is corroborated by the decline in slope, which indicates such a transition.

The diel vertical migration of zooplankton can induce errors in studies based on field sampling. In our study, one transect was sampled during approximately 2 h for short transects and 4 h for long transects. In the pre-intrusion period, transects 1–5 and 10–11 were sampled during the night (19:00–06:00), the others during the day. The vertical distributions of zooplankton on neighbouring transects did not indicate any diel vertical migration patterns, but coincided with the change of physical features rather than with sampling time (Figures 4 and 7). This observation is consistent with the findings of Falkenhaug et al. (1997), in which the vertical distribution of copepods off the north Norwegian coast was dominated

by seasonal rather than diel vertical migration. This was particularly evident during the period of midnight sun, where vertical behaviour was weak or absent. Błachowiak-Samołyk et al. (2006) also reported that Arctic zooplankton do not perform diel vertical migrations during periods of midnight sun.

The observed dynamics in the zooplankton community described by the size structure is consistent with our understanding of ecosystem functioning in these waters, where the peak of copepod biomass on the North Norwegian shelf break is reached as early as in May further west off Troms County, with subtle differences in zooplankton species assemblages and/or a different demography crossing the shelf in spring (Halvorsen & Tande 1999). Therefore, the biovolume spectrum change effectively depicts the intrusion of water hosting a zooplankton community with a different life-history stage distribution of the dominant copepod species (*Calanus finmarchicus*), or with more abundant smaller forms like *Oithona* spp., and *Oncea* spp. (Halvorsen & Tande 1999).

Numerous studies have addressed the internal dynamics of eddies from a 'bloom phase' to a 'decay phase' in order to reveal the underlying mechanisms for differences in zooplankton species, demography and vertical migration behaviour (McGillicuddy et al. 2007, Ledwell et al. 2008, Li & Hansell 2008). Our two surveys over these eddies were conducted in a period of 7 days between 15 and 22 May 2002, which was not long enough to observe the development of zooplankton communities with intruded populations. On the other hand, the wind event might have carried in capelin larvae that could have been retained in the long-lived eddy field off Varanger after our study. Stomach analyses of capelin larvae off the coast of Finnmark demonstrate that they prey upon invertebrate eggs, bivalves, copepod eggs, nauplii and copepodites (Pedersen & Fossheim 2008), an observation endorsed by findings from the Gulf of St. Lawrence (Vesin et al. 2006). The biovolume spectrum data indicate a larger standing stock of small size zooplankton and a smaller standing stock of large zooplankton after the wind event off the Cape. To what extent these changes in the zooplankton community were reflected in the upper trophic levels, especially the recruiting capelin larvae, cannot be determined. The overall effect of episodic wind events on the recruitment of capelin remains unknown and thus is still an open research question.

The formation of eddies on the North Norwegian shelf is linked primarily to topographic features, but their strength and persistence are strongly governed by tides, baroclinic fields and wind forcing. These topographically steered eddies generate a strong retention of zooplankton and fish larvae on the North Norwegian shelf (Zhu et al. 2009). In tracking zooplankton

cohorts and eddy studies, there are several methodological challenges to delineate internal processes of zooplankton community evolution such as growth and trophic dynamics, and exchange processes such as intrusions of other populations and migration behaviour over protracted time windows. For example, it is a challenge to map both mesoscale eddies and biological fields of plankton community structures synoptically. But it is probably more challenging to map the evolution of these eddies and plankton communities along their advection track. A combination of different technologies such as remote sensing, modelling and advanced instrument platforms will be instrumental in the future for studies of biological communities, and their evolution in time and space.

Acknowledgements

This work is a contribution to the Barents Sea Capelin and Herring – Coexistence or Exclusion (BASECOEX) research programme. A special ‘Thank you’ goes to the crew of r./v. ‘Jan Mayen’ for conducting the cruise and to Dr Sünnje Basedow for discussions.

References

- Benitez-Nelson C. R., Bidigare R. R., Dickey T. D., Landry M. R., Leonard C. L., Brown S. L., Nencioli F., Rii Y. M., Maiti K., Becker J. W., Bibby T. S., Black W., Cai W. J., Carlson C. A., Chen F., Kuwahara V. S., Maharrey C., McAndrew P. M., Quay P. D., Rappé M. S., Selph K. E., Simmons M. P., Yang E. J., 2007, *Mesoscale eddies drive increased silica export in the subtropical Pacific Ocean*, *Science*, 316 (5827), 1017–1021.
- Błachowiak-Samołyk K., Kwaśniewski S., Richardson K., Dmoch K., Hansen E., Hop H., Falk-Petersen S., Mouritsen L. T., 2006, *Arctic zooplankton do not perform diel vertical migration (DVM) during periods of midnight sun*, *Mar. Ecol.-Prog. Ser.*, 308, 101–116.
- Davis C. S., Wiebe P. H., 1985, *Macrozooplankton biomass in a warm-core Gulf Stream ring: time series changes in size structure, taxonomic composition, and vertical distribution*, *J. Geophys. Res.*, 90 (C5), 8871–8884.
- Dickie L. M., Kerr S. R., Boudreau P. R., 1987, *Size-dependent processes underlying regularities in ecosystem structure*, *Ecol. Monogr.*, 57 (3), 233–250.
- Eden B. R., Steinberg D. K., Goldthwait S. A., McGillicuddy Jr. D. J., 2009, *Zooplankton community structure in a cyclonic and mode-water eddy in the Sargasso Sea*, *Deep-Sea Res. Pt. I*, 56 (10), 1757–1776.
- Edvardsen A., Zhou M., Tande K. S., Zhu Y. W., 2002, *Zooplankton population dynamics: measuring in situ growth and mortality rates using an Optical Plankton Counter*, *Mar. Ecol.-Prog. Ser.*, 227, 205–219.

- Falkenhaug T., Tande K.S., Timonin A., 1997, *Spatio-temporal patterns in the copepod community in Malangen, Northern Norway*, J. Plankton Res., 19 (4), 449–468.
- Fossheim M., Zhou M., Tande K.S., Pedersen O.P., Zhu Y., Edvardsen A., 2005, *Interactions between biological and environmental structures along the coast of Northern Norway*, Mar. Ecol.-Prog. Ser., 300, 147–158.
- Gandin L., 1963, *Objective analysis for meteorological fields*, Gidromet, Leningrad, English translation: 1965, Israel Prog. Sci. Trans., Jerusalem, 242 pp.
- Gjevik B., Moe H., 1994, *Steady and transient flows around banks located near a shelf edge*, Cont. Shelf Res., 14 (12), 1389–1409.
- Goldthwait S.A., Steinberg D.K., 2008, *Elevated biomass of mesozooplankton and enhanced fecal pellet flux in cyclonic and mode-water eddies in the Sargasso Sea*, Deep-Sea Res. Pt. II, 55 (10–13), 1360–1377.
- Halvorsen E., Tande K.S., 1999, *Physical and biological factors influencing the seasonal variations in distribution of zooplankton across the shelf at Nordvestbanken, northern Norway, 1994*, Sarsia, 84 (3–4), 279–292.
- Herman A.W., Beanlands B., Phillips E.F., 2004, *The next generation of optical plankton counter: the Laser-OPC*, J. Plankton Res., 26 (10), 1135–1145.
- Hernández-León S., Almeida C., Gomez M., Torres S., Montero I., Portillo-Hahnefeld A., 2001, *Zooplankton biomass and indices of feeding and metabolism in island-generated eddies around Gran Canaria*, J. Marine Syst., 30 (1–2), 51–66.
- Jakobsen T., 1987, *Coastal cod in northern Norway*, Fish. Res., 5 (2–3), 223–234.
- Johannessen J.A., Shuchman R.A., Digranes G., Lyzenga D.R., Wackerman C., Johannessen O.M., Vachon P.W., 1996, *Coastal ocean fronts and eddies imaged with ERS 1 synthetic aperture radar*, J. Geophys. Res., 101 (C3), 6651–6667.
- Landry M.R., Decima M., Simmons M.P., Hannides C.C.S., Daniels E., 2008, *Mesozooplankton biomass and grazing responses to Cyclone Opal, a subtropical mesoscale eddy*, Deep-Sea Res. Pt. II, 55 (10–13), 1378–1388.
- Ledwell J.R., McGillicuddy Jr. D.J., Anderson L.A., 2008, *Nutrient flux into an intense deep chlorophyll layer in a mode-water eddy*, Deep-Sea Res. Pt. II, 55 (10–13), 1139–1160.
- Lewis D.M., Belcher S.E., 2004, *Time-dependent, coupled, Ekman boundary layer solutions incorporating Stokes drift*, Dynam. Atmos. Oceans, 37 (4), 313–351.
- Li Q.P., Hansell D.A., 2008, *Nutrient distributions in baroclinic eddies of the oligotrophic North Atlantic and inferred impacts on biology*, Deep-Sea Res. Pt. II, 55 (10–13), 1291–1299.
- Ljøen R., Nakken O., 1969, *On the hydrography of the shelf waters of Møre and Helgeland*, Fisk. Dir. Skr. Ser. Havunders., 15, 285–294.
- Loeng H., 1991, *Features of the oceanographic conditions of the Barents Sea*, Polar Res., 10 (1), 5–18.

- Mann K. H., Lazier J. R. N., 2006, *Dynamics of marine ecosystems*, Blackwell Publ., Malden, MA, 496 pp.
- McGillicuddy Jr. D. J., Anderson L. A., Bates N. R., Bibby T., Buesseler K. O., Carlson C. A., Davis C. S., Ewart C., Falkowski P. G., Goldthwait S. A., Hansell D. A., Jenkins W. J., Johnson R., Kosnyrev V. K., Ledwell J. R., Li Q. P., Siegel D. A., Steinberg D. K., 2007, *Eddy/wind interactions stimulate extraordinary mid-ocean plankton blooms*, *Science*, 316 (5827), 1021–1026.
- Orvik K. A., Mork M., 1995, *A case study of Doppler-shifted inertial oscillations in the Norwegian Coastal Current*, *Cont. Shelf Res.*, 15 (11–12), 1369–1379.
- Ottersen G., Sundby S., 1995, *Effects of temperature, wind and spawning stock biomass on recruitment of Arcto-Norwegian cod*, *Fish. Oceanogr.*, 4 (4), 278–292.
- Owen R., 1981, *Fronts and eddies in the sea: mechanisms, interactions and biological effects*, [in:] *Analysis of marine ecosystems*, A. R. Longhurst (ed.), Acad. Press, London, 197–233.
- Pedersen O. P., Gaardsted F., Lågstad P., Tande K. S., 2010, *On the use of the HUGIN 1000 HUS Autonomous Underwater Vehicle for high resolution zooplankton measurements*, *J. Oper. Oceanogr.*, 3 (1), 17–25.
- Pedersen O. P., Tande K. S., Pedersen T., Slagstad D., 2009, *Advection and retention as life trait modulators of capelin larvae – A case study from the Norwegian coast and the Barents Sea*, *Fish. Res.*, 97 (3), 234–242.
- Pedersen O. P., Zhou M., Tande K. S., Edvardsen A., 2005, *Eddy formation on the coast of North Norway – evidenced by synoptic sampling*, *ICES J. Mar. Sci.*, 62 (4), 615–628.
- Pedersen T., Fossheim M., 2008, *Diet of 0-group stages of capelin (*Mallotus villosus*), herring (*Clupea harengus*) and cod (*Gadus morhua*) during spring and summer in the Barents Sea*, *Mar. Biol.*, 153 (6), 1037–1046.
- Platt T., Denman K., 1978, *The structure of pelagic marine ecosystems*, *Rapp. P.-V. Réun. Cons. Int. Explor. Mer*, 173, 60–65.
- Price J. F., Weller R. A., Schudlich R. R., 1987, *Wind-driven ocean currents and Ekman transport*, *Science*, 238 (4833), 1534–1538.
- Rodriguez L., Mullin M. M., 1986, *Relation between biomass and body weight of plankton in a steady state oceanic ecosystem*, *Limnol. Oceanogr.*, 31 (2), 361–370.
- Sætre R., Ljøen R., 1971, *The Norwegian coastal current*, *Proc. First Int. Conf. Port and Ocean Engineering under Arctic conditions*, Vol. 2., Tech. Univ. Norway, Trondheim, 514–535.
- Sundby S., 1984, *Influence of bottom topography on the circulation at the continental shelf of northern Norway*, *Fisk. Dir. Skr. Ser. Havunders.*, 17, 501–519.
- Tsurumi M., Mackas D. L., Whitney F. A., DiBacco C., Galbraith M. D., Wong C. S., 2005, *Pteropods, eddies, carbon flux, and climate variability in the Alaska Gyre*, *Deep-Sea Res. Pt. II*, 52 (7–8), 1037–1053.

-
- Vesin J. P., Leggett W. C., Able K. W., 1981, *Feeding ecology of capelin (Mallotus villosus) in the estuary and western Gulf of St. Lawrence and its multispecies implications*, Can. J. Fish. Aquat. Sci., 38, 257–267.
- Wiebe P. P., 1988, *Functional regression equations for zooplankton displacement volume, wet weight, dry weight and carbon: A correction*, Fish. Bull, 86, 833–835.
- Wiebe P. H., Morton A. W., Bradley A. M., Backus R. H., Craddock J. E., Barber V., Cowles T. J., Flierl G. R., 1985, *New developments in the MOCNESS, an apparatus for sampling zooplankton and micronekton*, Mar. Biol., 87 (3), 313–323.
- Zhou M., 2006, *What determines the slope of a plankton biomass spectrum?*, J. Plankton Res., 28 (5), 437–448.
- Zhou M., Huntley M. E., 1997, *Population dynamics theory of plankton based on biomass spectra*, Mar. Ecol.-Prog. Ser., 159, 61–73.
- Zhou M., Tande K. S., Zhu Y., Basedow S., 2009, *Productivity, trophic levels and size spectra of zooplankton in northern Norwegian shelf regions*, Deep-Sea Res. Pt. II, 56 (21–22), 1934–1944.
- Zhu Y., Tande K. S., Zhou M., 2009, *Mesoscale physical processes and zooplankton productivity in the northern Norwegian shelf region*, Deep-Sea Res. Pt. II, 56 (21–22), 1922–1933.